

catalysts exhibit an apparent activation energy of ~ 60 kcal/mol for ethane formation.^{2,12-15} This value is approximately the same as that found for Li-doped MgO,^{2,12-15} although the activity of pure MgO is some 10-fold lower. The enhanced activity of Li-promoted MgO catalysts for ethane production is thus a predictable consequence of the increase in the density of F centers and F aggregates in the near-surface region which occurs following the addition of Li and MgO.

Acknowledgment. We acknowledge with pleasure the support of this work by the Gas Research Institute and the Department of Energy, Office of Basic Energy Sciences, Division of Chemical Science.

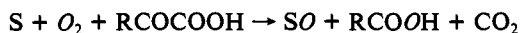
Model Complexes for α -Keto Acid-Dependent Enzymes. Structure and Reactivity of $[\text{Fe}^{\text{II}}[\text{tris}(6\text{-methyl-2-pyridyl)methyl}]\text{amine}](\text{benzoylformate})(\text{ClO}_4)$

Yu-Min Chiou and Lawrence Que, Jr.*

Department of Chemistry, University of Minnesota
Minneapolis, Minnesota 55455

Received March 2, 1992

α -Keto acid-dependent enzymes¹ catalyze a wide variety of reactions involving the oxidative decarboxylation of a keto acid concomitant with the functionalization of an unreactive C-H bond.² For hydroxylases, one atom from dioxygen is introduced into the substrate (S) and the other into the resulting carboxylic acid.³ Examples of this type of enzyme include prolyl 4-



hydroxylase,⁴ 4-hydroxyphenylpyruvate dioxygenase,⁵ and thymine hydroxylase.⁶ Fe(II) appears to be required for reactivity;^{7,8} however, little is known about the reaction mechanism or the coordination environment around the metal center. A plausible mechanism has been proposed in which the α -keto acid is oxidatively decarboxylated to produce a reactive intermediate, which then hydroxylates the susceptible substrate.⁹ This mechanism is supported by the uncoupling of the 2-oxoglutarate decarboxylation from hydroxylation in reactions catalyzed by proline,

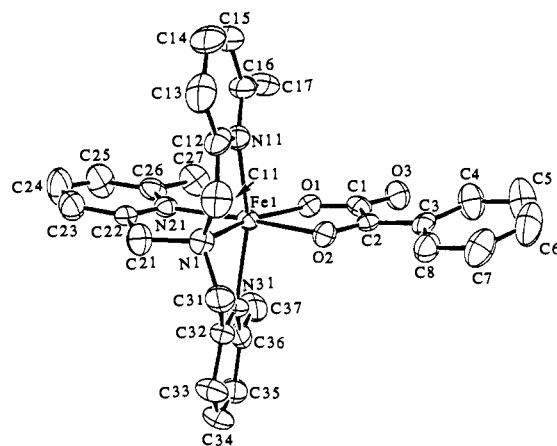


Figure 1. ORTEP view of $[\text{Fe}^{\text{II}}(\text{TLA})(\text{BF})]^+$, showing 50% probability thermal ellipsoids and atom labeling scheme. Hydrogen atoms are omitted for clarity. Selected bond distances (\AA) and angles ($^\circ$) are as follows: Fe-O1, 2.001 (4); Fe-O2, 2.212 (4); Fe-N1, 2.171 (5); Fe-N11, 2.273 (6); Fe-N21, 2.166 (5); Fe-N31, 2.231 (6); O1-Fe-O2, 75.3 (2); O1-Fe-N21, 118.7 (2); N1-Fe-N21, 81.3 (2); N1-Fe-O2, 84.7 (2); N11-Fe-N31, 153.3 (2).

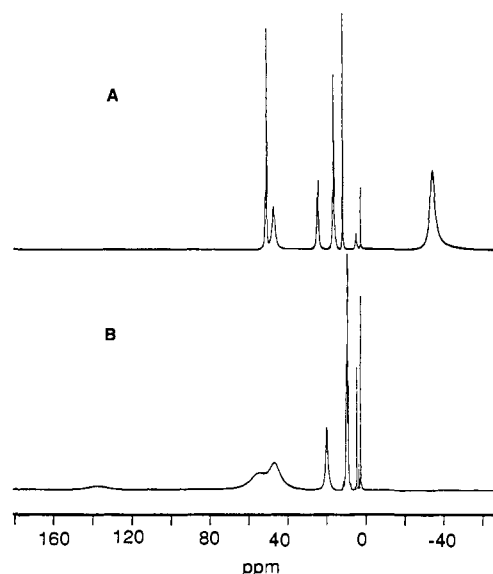


Figure 2. ^1H NMR spectra of **1** and **2** in CD_3CN . The peak assignments are deduced from peak integration and T_1 (ms) measurements. (A) $[\text{Fe}^{\text{II}}(\text{TLA})(\text{BF})](\text{ClO}_4)$ (**1**): BF *o*-H at 24 ppm (2.4 ms), *m*-H at 11 ppm (15 ms), and *p*-H at 16 ppm (~ 17 ms); TLA β -H at 50 ppm (7.3 ms) and 46 ppm (3.0 ms), γ -H at 16 ppm (~ 17 ms), α -CH₃ at -35 ppm (0.6 ms). (B) $[\text{Fe}^{\text{II}}(\text{TPA})(\text{BF})](\text{ClO}_4)$ (**2**): BF *o*-H at 9.0 ppm (4.5 ms), *m*-H at 8.6 ppm (32 ms), and *p*-H at 8.2 ppm (60 ms); TPA α -H at 137 ppm (1.1 ms), CH₂ at 53 ppm (2.4 ms), β -H at 46 ppm (8.4 ms), and γ -H at 20 ppm (22 ms).

γ -butyrobetaine, and thymine hydroxylases in the presence of substrate analogues.¹⁰ Herein, we report the synthesis of the first Fe^{II}- α -keto acid complexes, their physical properties, and their reactivity with dioxygen.

Treatment of $\text{Fe}(\text{ClO}_4)_2 \cdot 6\text{H}_2\text{O}$ with equimolar amounts of TLA¹¹ or TPA^{12,13} and benzoylformate (BF) in methanol affords

(1) For reviews, see: (a) Abbott, M. T.; Udenfriend, S. *Molecular Mechanisms of Oxygen Activation*; Hayaishi, O., Ed.; Academic Press: New York, 1974; Chapter 5. (b) Hanauske-Abel, H. M.; Günzler, V. *J. Theor. Biol.* **1982**, *94*, 421-455. (c) Townsend, C. A.; Basak, A. *Tetrahedron* **1991**, *47*, 2591-2602.

(2) Hamilton, G. A. *Prog. Bioorg. Chem.* **1971**, *1*, 83-157.

(3) Lindblad, B.; Lindstedt, G.; Tofft, M.; Lindstedt, S. *J. Am. Chem. Soc.* **1969**, *91*, 4604-4606.

(4) (a) Myllylä, R.; Kaska, D. D.; Kivirikko, K. I. *Biochem. J.* **1989**, *263*, 609-611. (b) Majamaa, K.; Günzler, V.; Hanauske-Abel, H. M.; Myllylä, R.; Kivirikko, K. I. *J. Biol. Chem.* **1986**, *261*, 7819-7823. (c) Majamaa, K.; Hanauske-Abel, H. M.; Günzler, V.; Kivirikko, K. I. *Eur. J. Biochem.* **1984**, *138*, 239-245. (d) Nietfeld, J. J.; De Jong, L.; Kemp, A. *Biochim. Biophys. Acta* **1982**, *704*, 321-325. (e) Tuderman, L.; Myllylä, R.; Kivirikko, K. I. *Eur. J. Biochem.* **1977**, *80*, 341-348 and 349-357.

(5) (a) Bradley, F. C.; Lindstedt, C.; Lipscomb, J. D.; Que, L., Jr.; Roe, A. L.; Rundgren, M. *J. Biol. Chem.* **1986**, *261*, 11693-11696. (b) Pascal, R. A., Jr.; Oliver, M. A.; Chen, Y. C. *J. Biochemistry* **1985**, *24*, 3158-3165. (c) Lindblad, B.; Lindstedt, G.; Lindstedt, S. *J. Am. Chem. Soc.* **1970**, *92*, 7446-7449. (d) Fellman, J. H.; Fujita, T. S.; Roth, E. S. *Biochim. Biophys. Acta* **1972**, *284*, 90-100.

(6) (a) Thornburg, L. D.; Stubbe, J. *J. Am. Chem. Soc.* **1989**, *111*, 7632-7633. (b) Holme, E.; Lindstedt, G.; Lindstedt, S.; Tofft, M. *J. Biol. Chem.* **1971**, *246*, 3314-3319.

(7) (a) Günzler, V.; Majamaa, K.; Hanauske-Abel, H. M.; Kivirikko, K. I. *Biochim. Biophys. Acta* **1986**, *873*, 38-44. (b) De Jong, L.; Kemp, A. *Biochim. Biophys. Acta* **1982**, *709*, 142-145.

(8) (a) Lindstedt, S.; Rundgren, M. *J. Biol. Chem.* **1982**, *257*, 11922-11931. (b) Denum, J.; Lindstedt, S.; Rundgren, M. *Oxidases Relat. Syst., Proc. Int. Symp.*, **3rd** **1982**, 519-542.

(9) Holme, E.; Lindstedt, S. *Biochim. Biophys. Acta* **1982**, *704*, 278-283.

(10) (a) Counts, D. F.; Cardinale, G. J.; Udenfriend, S. *Proc. Natl. Acad. Sci. U.S.A.* **1978**, *75*, 2145-2149. (b) Roe, N. V.; Adams, E. *J. Biol. Chem.* **1978**, *253*, 6327-6330. (c) Holme, E.; Lindstedt, S.; Nordin, I. *Biochem. Biophys. Res. Commun.* **1982**, *107*, 518-524. (d) Holme, E.; Lindstedt, S.; Nordin, I. *Biosci. Rep.* **1984**, *4*, 433-440. (e) Holme, E.; Lindstedt, G.; Lindstedt, S. *Acta Chem. Scand. Ser. B* **1979**, *33*, 621-622.

(11) De Mota, M. M.; Rodgers, J.; Nelson, S. M. *J. Chem. Soc. A* **1969**, 2036-2044.

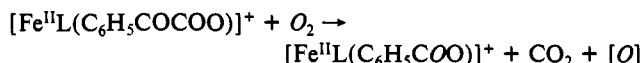
(12) Gafford, B. G.; Holwerda, R. A. *Inorg. Chem.* **1989**, *28*, 60-66.

(13) Abbreviations used: BF, benzoylformate; OAc, acetate; OBz, benzoate; TPA, tris(2-pyridylmethyl)amine; TLA, tris(6-methyl-2-pyridylmethyl)amine.

complexes $[\text{Fe}^{\text{II}}(\text{TLA})(\text{BF})](\text{ClO}_4)$ (**1**) and $[\text{Fe}^{\text{II}}(\text{TPA})(\text{BF})](\text{ClO}_4)$ (**2**), respectively.¹⁴ The X-ray structure of **1**¹⁵ shows that the complex is a distorted octahedron featuring a tetradentate TLA and a bidentate BF ligand (Figure 1). The BF ligand is coordinated to the iron center via the carboxylate oxygen (O1) at 2.001 (4) Å and the carbonyl oxygen (O2) at 2.212 (4) Å; the 0.21-Å bond length difference is probably due to the greater basicity of the carboxylate, and the phenyl group is nearly coplanar with the α -keto acid moiety. Steric interactions between the C27 α -methyl group and the corresponding C17 and C37 groups on the TLA ligand result in Fe-N11 and Fe-N31 distances which are ca. 0.1 Å longer than the Fe-N1 and Fe-N21 distances. Furthermore, the BF ligand is pushed away from the pyridine in the same plane, giving rise to an O1-Fe-N21 angle of 118.7 (2)°.

The UV-visible spectrum of **1** exhibits features at 370 (ϵ 2400 $\text{M}^{-1} \text{cm}^{-1}$), 544 (ϵ 690 $\text{M}^{-1} \text{cm}^{-1}$), and 590 nm (sh, ϵ 600 $\text{M}^{-1} \text{cm}^{-1}$) in CH_3CN , which gives **1** its unusual purple-blue color. Its ¹H NMR spectrum (Figure 2A) shows large isotropic shifts for the BF protons due to delocalization of unpaired spin density through the coordinated carbonyl. In contrast, the analogous TPA complex **2** is yellow in color ($\lambda_{\text{max}} = 385 \text{ nm}$, ϵ 2400 $\text{M}^{-1} \text{cm}^{-1}$), and the BF protons are in the diamagnetic region (8–9 ppm, Figure 2B). The loss of color and the small BF paramagnetic shifts suggest that the BF carbonyl oxygen in **2** is not coordinated to the iron center.

Both **1** and **2** react with O_2 in CH_3CN under ambient conditions according to



affording benzoic acid in nearly quantitative yield (98% for **1** and 96% for **2** by GC).¹⁶ The reaction of O_2 with **1** proceeds over a 1-week period; ¹H NMR analysis of the reaction solution indicates the nearly quantitative formation of $[\text{Fe}^{\text{II}}(\text{TLA})(\text{OBz})]^+$ (**3**), whose properties are corroborated by independent synthesis.¹⁷ When the reaction is carried out in the presence of 10 equiv of 2,4-di-*tert*-butylphenol, 0.75 mol of the corresponding biphenol is formed per mole of ferrous complex (by NMR) without altering the yield of the product complex. We can thus trap most of the oxidizing equivalents implied by [O] in the reaction scheme above. The reaction of O_2 with **2**, on the other hand, requires 2 days and affords near-stoichiometric amounts of $[\text{Fe}^{\text{III}}\text{O}(\text{OBz})_2(\text{TPA})_2]^{2+}$ (**4**),¹⁸ which results from the further oxidation of the resultant $[\text{Fe}^{\text{II}}(\text{TPA})(\text{OBz})]^+$ complex.¹⁹

(14) Complexes **1** and **2** were obtained by combining equimolar amounts (0.5 mmol) of TLA or TPA, benzoylformic acid, Et_3N , and $\text{Fe}(\text{ClO}_4)_2 \cdot 6\text{H}_2\text{O}$ in 10 mL of CH_3OH under argon. The solid products obtained by cooling and subsequent filtration corresponded to yields of 78% and 85%, respectively. Elemental analysis for $[\text{Fe}^{\text{II}}(\text{TLA})(\text{BF})](\text{ClO}_4)$ (**1**). Anal. Calcd for $\text{C}_{29}\text{H}_{29}\text{ClFeN}_4\text{O}_7$: C, 54.69; H, 4.59; N, 8.80; Cl, 5.57. Found: C, 54.44; H, 4.76; N, 8.65; Cl, 5.39. Elemental analysis for $[\text{Fe}^{\text{II}}(\text{TPA})(\text{BF})](\text{ClO}_4)$ (**2**). Anal. Calcd for $\text{C}_{28}\text{H}_{23}\text{ClFeN}_4\text{O}_7$: C, 52.50; H, 3.90; N, 9.42. Found: C, 52.54; H, 4.17; N, 9.18. Caution: Perchlorate salts are potentially explosive and should be handled with care.

(15) Diffraction quality crystals of $[\text{Fe}(\text{TLA})(\text{BF})](\text{ClO}_4)$ were obtained from acetone/diethyl ether. The complex crystallizes in the triclinic system, space group $P\bar{1}$, with $a = 8.931$ (6) Å, $b = 13.366$ (7) Å, $c = 15.160$ (7) Å, $\alpha = 75.92$ (4)°, $\beta = 81.06$ (5)°, $\gamma = 70.78$ (5)°, $V = 1652$ (4) Å³, and $Z = 2$. With the use of 6481 unique observed reflections, for which $I_{\text{obsd}} > 3.0\sigma(I)$, collected at 172 K with Mo K α ($\lambda = 0.71069$ Å) radiation out to $2\theta_{\text{max}} = 51.9^\circ$ on an Enraf-Nonius CAD-4 X-ray diffractometer, the structure was solved by direct methods and refined to $R = 0.071$ and $R_w = 0.082$.

(16) Oxygenation reactions were run on a 0.1-mmol scale in 20 mL of CH_3CN under ambient conditions. The amount of benzoic acid was quantified by GC following the addition of 3 N HCl to the reaction solution and ether extraction.

(17) FAB-MS: m/z 509.3, corresponding to $[\text{Fe}^{\text{II}}(\text{TLA})(\text{OBz})]^+$. **3** exhibits NMR features at 43 (OBz α -H), 23 (OBz m -H), 14 (OBz p -H), 51 (TLA β -H), 12 (TLA γ -H), and -50 ppm (TLA α -CH₃), as found for the authentic complex $[\text{Fe}^{\text{II}}(\text{TLA})(\text{OBz})](\text{ClO}_4)$ (Zang, Y., unpublished data). The conversion of **1** to **3** was monitored by NMR by integration of the α -methyl protons of TLA of the two complexes.

(18) FAB-MS: m/z 1049, corresponding to $[\text{4}(\text{ClO}_4)]^+$. **4** exhibits NMR features at 33 (broad, TPA α -H and/or CH₂), 16 (TPA β -H), 8 (TPA γ -H), and 8–9 ppm (OBz protons), which are similar to the features found for $[\text{Fe}^{\text{III}}\text{O}(\text{TPA})_2(\text{OAc})_2]^{2+}$.¹⁹

¹⁸O₂ labeling studies of the reaction of **1** and **2** with O_2 show the incorporation of one atom of ¹⁸O into the benzoate product, as has been observed for corresponding enzymatic reactions,^{6b,20} but only one-half of the product molecules are labeled. This incomplete labeling result is likely due to the loss of label from solvent exchange, as a parallel ¹⁶O₂ reaction with **2** carried out in the presence of trace amounts of H₂¹⁸O shows the incorporation of as many as five atoms of ¹⁸O into complex **4**. Further mechanistic investigations are in progress.

In summary, **1** and **2** represent the first complexes to model putative Fe(II)-cofactor interactions for α -keto acid-dependent enzymes. Both complexes undergo nearly quantitative oxidative decarboxylation upon exposure to dioxygen and thus serve as a useful starting point for understanding the bioinorganic chemistry of these fascinating enzymes.

Acknowledgment. We are grateful to Professor J. D. Britton for his expertise in the X-ray diffraction experiments and Dr. Yanhong Dong for the synthesis of TLA. This work has been supported by the National Institutes of Health (GM-33162).

Supplementary Material Available: Tables of the atomic coordinates, thermal parameters, bond lengths, and bond angles for $[\text{Fe}^{\text{II}}(\text{TLA})(\text{BF})](\text{ClO}_4)$ (14 pages). Ordering information is given on any current masthead page.

(19) We have shown that the corresponding $[\text{Fe}^{\text{II}}(\text{TPA})(\text{OAc})_2]^{2+}$ complex readily autoxidizes to yield $[\text{Fe}^{\text{III}}\text{O}(\text{TPA})_2(\text{OAc})_2]^{2+}$. Menage, S.; Zang, Y.; Hendrich, M. P.; Que, L., Jr. *J. Am. Chem. Soc.*, in press.

(20) (a) Lindblad, B.; Lindstedt, G.; Lindstedt, S. *J. Am. Chem. Soc.* **1970**, *92*, 7446–7449. (b) Siegel, B. *Bioorg. Chem.* **1979**, *8*, 219–226.

Catalytic Asymmetric Dihydroxylation of Cis-Disubstituted Olefins

Lisa Wang[†] and K. Barry Sharpless^{*‡}

Departments of Chemistry
Massachusetts Institute of Technology
Cambridge, Massachusetts 02139
The Scripps Research Institute
La Jolla, California 92037

Received May 12, 1992

Since the inception of the osmium-catalyzed asymmetric dihydroxylation (AD) in 1988,¹ substantial progress has been attained in the development of ligands that generate ever higher levels of enantioselectivity.² With the advent of the dihydroquinidine (DHQD) and dihydroquinine (DHQ) phthalazine ligands, (DHQD)₂-PHAL and (DHQ)₂-PHAL, enantiomeric excesses (ee's) of greater than 90% are realized with four of the six possible olefin substitution patterns, namely, the mono-, geminal-di-, trans-di-, and trisubstituted olefins (Chart I).³

[†] Massachusetts Institute of Technology.

[‡] The Scripps Research Institute.

(1) Jacobsen, E. N.; Markó, I.; Mungall, W. S.; Schröder, G.; Sharpless, K. B. *J. Am. Chem. Soc.* **1988**, *110* (6), 1968–1970.

(2) (a) Sharpless, K. B.; Amberg, W.; Beller, M.; Chen, H.; Hartung, J.; Kawanami, Y.; Lübben, D.; Manoury, E.; Ogino, Y.; Shibata, T.; Ukita, T. *J. Org. Chem.* **1991**, *56* (15), 4585–4588. (b) Wai, J. S. M.; Markó, I.; Svendsen, J. S.; Finn, M. G.; Jacobsen, E. N.; Sharpless, K. B. *J. Am. Chem. Soc.* **1989**, *111* (13), 1123–1125. (c) Kwong, H.-L.; Sorato, C.; Ogino, Y.; Chen, H.; Sharpless, K. B. *Tetrahedron Lett.* **1990**, *31*, 2999–3002. (d) Shibata, T.; Gilheany, D. G.; Blackburn, B. K.; Sharpless, K. B. *Tetrahedron Lett.* **1990**, *31* (27), 3817–3820. For other examples of catalytic asymmetric oxidations of cis-disubstituted olefins, see: (e) Jacobsen, E. N.; Zhang, W.; Muci, A. R.; Ecker, J. R.; Deng, L. *J. Am. Chem. Soc.* **1991**, *113*, 7063–7064. (f) Zhang, W.; Loebach, J. L.; Wilson, S. R.; Jacobsen, E. N. *J. Am. Chem. Soc.* **1990**, *112* (7), 2801–2803. (g) Zhang, W.; Jacobsen, E. N. *J. Org. Chem.* **1991**, *56* (7), 2296–2298. (h) Irie, R.; Noda, K.; Ito, Y.; Matsumoto, N.; Katsuki, T. *Tetrahedron Lett.* **1990**, *31* (50), 7345–7348.

(3) Sharpless, K. B.; Amberg, W.; Bennani, Y. L.; Crispino, G. A.; Hartung, J.; Jeong, K. S.; Kwong, H.-L.; Morikawa, K.; Wang, Z. M.; Xu, D.; Zhang, X.-L. *J. Org. Chem.* **1992**, *57* (10), 2768–2771, and references cited therein.